arXiv:cond-mat/9708136v1 [cond-mat.soft] 19 Aug 1997

Energy Dissipation and Trapping of Particles Moving on a Rough Surface

C. Henrique[1], M.A. Aguirre[2], A. Calvo[2], I. Ippolito[1], S. Dippel[3], G. G. Batrouni[4] and D. Bideau[1]

[1] *Groupe Matière Condensée et Matériaux (UMR 6626 au CNRS), Université de Rennes I, Bât. 11B, Campus de Beaulieu, 35042 Rennes Cedex, France.*

[2] *Facultad de Ingeniería. Paseo Colón 850, Buenos Aires, Argentina.*

[3] *Höchstleistungsrechenzentrum, Forschungszentrum Jülich, 52425 Jülich, Germany*

[4] *Institut Non-Linéaire de Nice, Université de Nice-Sophia Antipolis, 1361 route des Lucioles, 06560 Valbonne, France*

We report an experimental, numerical and theoretical study of the motion of a ball on a rough inclined surface. The control parameters are D, the diameter of the ball, θ, the inclination angle of the rough surface and E_{ki}, the initial kinetic energy. When the angle of inclination is larger than some critical value, $\theta > \theta_T$, the ball moves at a constant average velocity which is independent of the initial conditions. For an angle $\theta < \theta_T$, the balls are trapped after moving a certain distance. The dependence of the travelled distances on E_{ki}, D and θ. is analysed. The existence of two kinds of mechanisms of dissipation is thus brought to light. We find that for high initial velocities the friction force is constant. As the velocity decreases below a certain threshold the friction becomes viscous.

I. INTRODUCTION

Essentially due to the non linear and dissipative character of their interactions, flowing grains exhibit a range of complex and fascinating behaviour such as density waves [1], avalanches [2], arching [3] and segregation [4]. The energy exchange among the grains and between grains and walls are particularly important, but not well understood. The solid friction force itself is still an open problem [5] dating back to the work of Coulomb. In addition, the collective effects of this solid friction in a quasistatic deformation of a granular solid are not well understood [6]. To take into account the energy loss during collisions, we use only a very empirical parameter -the restitution coefficient- even if experiments [7] have shown that this coefficient is more complex than expected.

We have performed several experiments [8] on the motion of balls on rough inclined planes. One of our most important results is that in a regime characterized by an average constant velocity V, the macroscopic friction force is "viscous", i.e. proportional to V. In the $D-\theta$ parameter space, where D is the diameter of the moving ball and θ the inclination angle, the constant velocity regime, which we call regime B, is sandwitched between a decelerated/trapping regime A (for small D and/or θ) and a regime C in which the ball jumps on the plane, and eventually can reach a chaotic motion [9]. In this paper, we focus on how the ball losses its energy in the decelerated/trapping regime, A.

After a short description of the experimental procedure, we present results of the stopping distance of balls reached with low initial kinetic energy, as well as results from an approximate two dimensional stochastic model. We discuss energy dissipation in section III, and in the last section we propose a phenomenological model and compare it with numerical simulation.

II. EXPERIMENTAL PROCEDURE

The experimental setup used in this work has been described in detail elsewhere [10,11]. A rough plane is constructed by sticking particles (see below) on an adhesive surface. This surface is placed on a thick glass plane supported by a metal frame to prevent warping and a jack that allows the accurate adjustment and measurement of the angle of inclination, θ, which is one of the control parameters in our experiment. The rough surface is made of a monolayer of sifted rolled sand grains with mean radius, r, $0.2\text{mm} \leq r \leq 0.25\text{mm}$. These grains are glued to the adhesive surface in such a way as to obtain a homogeneous geometrically disordered rough surface with a surface fraction compacity close to 0.8. We used this surface to study the motion of steel spheres of diameter $1.6\text{mm} \leq D \leq 10.3\text{mm}$.

In order to control the initial kinetic energy supplied to the ball (i.e. the initial speed with which the ball hits the rough surface) a thin smooth plastic sheet is placed on the rough surface in the region where the ball is launched. A set of parallel and equally spaced lines is drawn on the sheet perpendicular to the direction of maximum slope of the plane. The first line is drawn at a distance equal to the smallest rolling ball radius, from the edge of the sheet nearest to the rough surface. To study the behavior of rolling balls with very low initial kinetic energy, $E_{ki} \approx 0$, we release them from this first line. To increase the initial E_{ki}, we simply release the ball from one of the other lines traced

higher up on the plane. It is then trivial to see that $E_{ki} \propto X_i$, where X_i is the distance travelled over the smooth surface.

The experimental procedure is as follows. The inclination angle of the plane is fixed at a desired value, and a straight barrier is placed at the location which gives the desired initial kinetic energy,E_{ki}. Twenty balls of a given radius, R, are positioned on the barrier on the uphill side and not touching each other. Removing the barrier, the balls are accelerated as they move the same distance, X_i, on the smooth surface, arriving at the rough surface with the same initial kinetic energy, E_{ki}. Since we have set the inclination angle, θ, in the range corresponding to the pinning regime, A, the released balls will come to a stop on the rough plane at various distances L_i. The susbscript i denotes a particular pinned ball. This procedure is repeated 35 times with the same experimental settings to collect statistics. We then repeat the experiment for different values of E_{ki}, R and θ, always keeping θ in the pinning regime. The uncertainty in length measurements is of the order of ± 1 mm and the number of balls for each set of parameters values investigated is large enough to have good statistics.

III. STOPPING DISTANCE OF BALLS WITH LOW INITIAL KINETIC ENERGY

With the method described above, we measured the distance, L_i, travelled on the rough surface by each ball and for a wide range of control parameter values (1.6mm $\leq D \leq$ 10.6mm and $1.5^\circ \leq \theta \leq 12.5^\circ$). In all cases X_i is taken as small as possible, around 2 mm. In Figs. 1 (a, b) typical L_i distributions are shown for $D = 2$mm and $\theta = 3^\circ$ and 5° respectively. It can be seen that these distributions peak for a travelled distance, L_i, of the order of the diameter of the moving ball (2mm). The distributions decay for larger values of the travelled distance, the decay being faster for the smaller θ.

We found that the decay of these distributions for the larger values of L_i is well fitted by an exponential

$$N = N_0 e^{-\alpha L_i}. \tag{3.1}$$

The solid lines in Figs. 1(a) and (b) are fits obtained with $\alpha = 2.9\text{cm}^{-1}$ and 0.5cm^{-1} respectively. Similar exponential distributions were found for the stopping distance by Riguidel *et al*, [8], but working under experimental conditions corresponding to regime B, where the moving ball reaches a steady, albeit fluctuating, velocity. In this regime, the balls are occasionally stopped by large holes on the surface. Their results were well fitted with α varying with θ as:

$$\alpha = exp\left(-aD^3 \sin^2\theta\right), \tag{3.2}$$

where a is a constant.

In order to complete and verify this law, we have performed a systematic study of the variations of α with θ. In Fig. 2 we show α as a function of θ for $D = 2$mm. Similar results were found for all the D values studied. Two different dependences are observed: A linear variation with large negative slope for inclination angles lower than 4° followed by a crossover to a different smoothly decreasing curve tending to zero for angles larger than 5°. Good agreement was found using eqn. 3.2 for this last part of the curve, as shown in the figure (solid line). However, it is clear that eqn. 3.2 is not valid for θ values smaller than 4°. This clearly demonstrates the existence of a change in the trapping mechanism of the rolling ball when the inclination angle goes from a value lower than 4° to a larger one. To find the angle at which the first trapping mechanism disappears, we look for the intercept of the straight line in Fig. 2 with the x-axis. We define this transition angle, θ_T, $\alpha = 0$ as the angle for which the trapping mechanism of regime A has disappeared. In Fig. 2, $\theta_T = 4.6^\circ$. This value is very close to that found previously [10] for the angle θ_{AB} at which the transition between the decelerated regime (regime A) and the mean constant velocity one (regime B) occurs (for the same D). In the same way, we can find the angles θ_T corresponding to $\alpha = 0$, for all studied D values. These θ_T angles can be compared with the θ_{AB} values previously reported [10]. Very good agreement is obtained for large D values, and slight differences for smaller ones.

We can therefore conclude that there are two trapping mechanisms: One due to large wells (disorder) in the surface, and the other one to *dissipation* (controlled to a large degree by the relative smoothness seen by the rolling ball). The measurement of the dependence of α on θ described above, provides a more physical and precise criterion for determining experimentally the transition line between these two regimes.

The fact that in Fig. 2 the transition between the two observed behaviours according to θ values occurs smoothly indicates that near the transition, *both* trapping mechanisms are important.

In fact, this experimental distribution of the stopping distances and their exponential fits was predicted using a

simple two dimensional[1] stochastic model. The above experimental verification came later. In this model one starts with Newton's equations of motion for the moving balls which are then simplified by making some approximations motivated by the geometry of the collisions and the properties of the dissipation. The resulting model describes well the statistical properties (i.e. averages and distributions) of physical quantities of the moving balls. For details of the model see reference [12]. In Fig. 3 we show the α versus θ plot obtained from the stochastic model. We see that it has the same form and functional dependence as that found in the experiments. The actual values of α and θ given by the model differ from the experimental ones. The model is too simple to give accurate quantitative predictions, for example rotation is ignored. However, the excellent qualitative agreement between the predictions and the experimental results means that the role of geometry, which is emphasized in the model is indeed crucial.

We define the median, L^*, of the stopping distance distribution as the length for which 50% of the balls are trapped on the rough surface. Since we found exponential distributions in all cases we have studied, we can write L^* as:

$$L^* = \frac{|\ln(0.5)|}{\alpha}. \tag{3.3}$$

As seen in Fig. 2 $\alpha = -a\sin(\theta) + b$, and from the definition of θ_T, $\alpha(\theta_T) = 0$, we see that $\alpha_{\theta\to\theta_T} = a(\theta - \theta_T)\cos(\theta_T)$, and therefore $L^*_{\theta\to\theta_T} \propto \frac{1}{|\theta-\theta_T|}$. Thus, L^* diverges for $\theta \to \theta_T$ in a way reminiscent of a phase transition with a critical exponent equal to unity.

In order to verify this behaviour we measure L^* for the distributions corresponding to different pairs of control parameter values (θ, D). In Fig. 4 the dependence of L^* on θ is shown for three D values. For $D = 10.3$mm the transition between regimes A and B occurs at $\theta = 2.5^\circ$ and for $D = 3$mm at $\theta = 4.4^\circ$. In both cases the very rapid increase of L^* as $\theta \to \theta_T$ from below, demonstrates an approximate divergence consistent with the above discussion. Let us recall, that as $\theta \to \theta_T$ we have *two* competing pinning mechanisms and therefore no true divergence. This "divergence" was based on the idealization that as we approach θ_T from below, pinning in regime A completely disappears. For the smallest D value shown in the figure ($D = 1.6$mm), the agreement between the proposed functional dependence of L^* on θ and the experimental results is also clear, even if the A-B transition is not yet reached.

IV. ENERGY DISSIPATION IN REGIME A

In this section we discuss energy dissipation in regime A, i.e. small angles of inclination, θ, where the balls always come to rest. With this goal in mind, balls were released from the various lines marked on the plastic sheet, as described in section II. In this way, controlled initial kinetic energies were supplied to the balls, and their stopping distances were studied.

We will first show that the transition A-B is not affected by the initial kinetic energy. This is in agreement with previous characterization of regime B as that interval of inclination angles for which the balls reach an average steady state velocity *independent* of the initial velocity (or kinetic energy). [12–14] We then analyze, for a very small inclination angle ($\theta = 2^\circ$), the stopping distance distributions for different initial kinetic energies and several D values. After that, we investigate the dependence of the mean distance travelled by the ball with its initial velocity. Finally, we propose a phenomenological interpretation of the experimental results obtained.

A. Experimental results

To study the influence of the initial velocity (V_i) on the transition between regimes A and B, 100 balls of diameter $D = 3$mm were released from $X_i = 0.3$ cm ($V_i \approx 5$ cm/s) and then from $X_i = 20$ cm ($V_i \approx 45$ cm/s). The stopping distance of each ball was measured, and L^* calculated. This procedure was repeated for ten different inclination angles of the rough surface, $2.7^\circ \leq \theta \leq 6^\circ$, in order to insure the change of the dynamical regime.

We have shown before that, with its rapid increase ("divergence"), L^* itself characterizes the transition. In Fig. 5 we show this divergence of L^* as a function of the inclination angle for the two values of the initial velocity, $V_i = 5, 45$ cm/s. It is clear that the A-B transition occurs at the same angle for both curves independently of V_i. This is so even though the initial velocity has a great influence on the travelling distance in regime A.

[1]The experiments are, of course, three dimensional: The two directions defining the rough plane, and the direction perpendicular to it.

We now discuss the evolution of the distribution of stopping distances as a function of the initial kinetic energy of the balls. The experimental procedure is as follows: The control parameters (θ and D) were fixed at values corresponding to regime A and a large enough number of balls were released at different X_i. The distance travelled by every ball before being trapped was measured. We show the distributions for the stopping distances in Fig. 6 for $D = 10.3$mm, $\theta = 2^\circ$ and four values of V_i. The distributions are essentially the same, except that the location of their centers moves towards increasing values of the travelled distance as the initial velocity is increased. The dispersion is very small.

We observe experimentally that those balls which begin their motion with larger initial velocity travel a longer distance before getting trapped. Moreover, balls released from the same X_i (i.e. the same initial velocity) move through almost the same distance on the rough surface before getting trapped over a distance of a few centimeters: The dispersion of the distribution of stopping distances is very small. This leads us to postulate that the ball does not get trapped unless its velocity is under some threshold value. To arrive at this value, it must first travel a certain distance on the rough surface to dissipate enough energy. Using a video camera and image processing, we were able to evaluate this threshold value. We launch several balls ($D = 6$mm, $\theta = 2^\circ$) with different initial kinetic energies ($0.5\text{cm} \leq X_i \leq 18.5\text{cm}$) and for each ball, the velocity is measured every acquired frame (15 frames by second). Balls travel a distance of about 15 cm before getting trapped. Our measurements indicate that balls do not get trapped while their speed exceeds 3 cm/s. Note that the velocity below which the ball can be trapped is independant of the initial velocity[2]. Since the distributions of stopping distances are rather narrow and symmetric, the average value $\tilde{L}$ is a good variable to use to characterize the energy loss. We show in Fig. 7 a plot of $\tilde{L}$ as a function of X_i, for $\theta = 2^\circ$ and $D = 10.3,$ and 4.7mm.

The first thing to notice is that $\tilde{L}$ increases with the initial kinetic energy ($\propto X_i$) of the balls. We also see that for $D = 10.3$mm and $X_i > 10$ cm, this dependence is linear. On the other hand, for $0\text{cm} \leq X_i \leq 10\text{cm}$, $\tilde{L}$ increases with X_i following another law. Note that for $X_i = 0$, $\tilde{L}$ must be 0. The same behaviour is seen for $D = 4.7$mm but, in this case, the crossover between the two dependences is around $X_i = 2$ cm.

The presence of two different behaviours for the stopping distance as a function of the initial kinetic energy suggests a change of the nature of the friction force between the two regimes. At the moment we cannot characterize these forces any further. However, in previous work [8,12,10,11], which concentrated on regime B, friction mechanisms were extensively studied experimentally, numerically and theoretically. Only three types of friction force are possible: $F = K_1$, $F = K_2 V$ and $F = K_3 V^2$. In the following section we use these experimental results to propose a phenomenological model with few parameters which reproduce the experimental results.

B. Physical model

Our objective is to describe the dynamics of a ball moving down a rough slightly inclined surface. Taking into account the experimental results just described, we can assume that two different types of friction forces exist. Which type of force enters into play depends, among other things, on the initial velocity of the ball. It is clear that when moving down the plane, a ball loses its initial energy by collisions and friction with the surface grains and finally is trapped. However, not much is known about the way in which this occurs. In particular, nothing is known about the average velocity as a function of the distance travelled. So, the main assumptions of our model are: (a) it is possible to define such a velocity function, $V(D)$, for all balls, and (b) to get trapped, V must be smaller than a certain threshold value V_{min}. In other words, we are assuming that to decrease its velocity from a value V_0 to a smaller one V_1, a ball has to travel the same distance λ_{01} independent of its initial velocity.

As for $V(D)$ we know that: $V(0) = V_i$ and we assume that $V(L) \leq V_{min}$ where V_i is the initial velocity of the ball and L is the corresponding trapping distance. Clearly, since the physical quantities of interest are fluctuating quantities given by some distribution, the quantities entering in the model are statistical averages.

With the above considerations, we can write:

$$\widetilde{L_0} = \widetilde{L_1} + \widetilde{\lambda_{01}}, \tag{4.1}$$

where $\widetilde{L_0}$ and $\widetilde{L_1}$ are the average stopping distances of balls released with initial velocities V_0 and $V_1 < V_0$, respectively, and $\widetilde{\lambda_{01}}$ is the mean distance travelled by the first set of balls as their velocity decreases from V_0 to V_1. Differentiating this equation with respect to V^2, we obtain:

[2]The same experiment was performed for $D = 6$mm, and $\theta = 2.85^\circ$ the threshold obtained in this case is 6.5 cm/s.

$$\frac{\partial \widetilde{\lambda(V)}}{\partial V^2} = -\frac{\partial \widetilde{L(V)}}{\partial V^2} \tag{4.2}$$

The right hand side of eqn. 4.2 may be evaluated from the experimental results presented in the previous section (Fig. 7). As we have already mentioned, for large enough initial kinetic energies, the dependence of $\tilde{L}$ on V^2 is linear. Therefore, eqn. 4.2 leads to: $\partial V^2/\partial \widetilde{\lambda(V)} =$ constant. This is the energy gradient and in consequence must be equal to the force. We thus find that, at large enough velocities, a ball moving down a rough surface suffers a constant friction force, $F = mK$, and that the experimental determination of $\widetilde{L(E_{ki})}$ provides a way to evaluate it.

On the other hand, for smaller initial kinetic energies we have found a different relation between $\tilde{L}$ and V^2 which, in fact, implies another mechanism for energy dissipation. In this case, we assume a viscous type friction force (i.e. proportional to the velocity). For each pair of values (θ, D), we define a velocity, V_l, for which the crossover between the two types of frictional forces occurs.

In other words, we propose that a ball of diameter D, moving down a rough surface made of grains of mean radius r, and inclined an angle θ, suffers a constant dissipation force ($F = mK$), while its velocity V is larger than $V_l(\theta, D)$; a viscous type dissipation force ($F = maV$) when its velocity is between $V_l(\theta, D)$ and $V_{min}(\theta, D)$, and that it gets trapped on the rough surface only if $V \leq V_{min}(\theta, D)$.

To verify these assumptions, we calculate the distances travelled given by the above model and compare them to the experimental ones. If a ball is released with a velocity $V > V_l$, the distance it travels according to this model is easily calculated to be

$$\widetilde{L(V)} = \frac{1}{2K}\left(V^2 - V_l^2\right) + \frac{V_l}{a}\left(1 - \frac{V_{min}}{V_l}\right). \tag{4.3}$$

On the other hand, if the release velocity, V, is less than V_l, the distance travelled is

$$\widetilde{L(V)} = \frac{V}{a}\left(1 - \frac{V_{min}}{V}\right). \tag{4.4}$$

We arrive then, at two equations with four parameters: a, K (which characterize the friction forces), V_{min} and V_l.

Using eqn. 4.2, $K(D)$ was calculated by fitting to the linear part of the $\tilde{L}$ versus V_i^2 curves, as explained just after Eqn. 4.2. Since the slopes of the linear regions in Fig. 7 depend on D, K is then a function of D. To determine a and V_{min} we fit Eqn. 4.4 to the curved regions (small X_i) of Fig. 7. However, in this region, we have enough data for such a fit only for $D = 10.3$mm, which is what we use. We note that for small X_i (small initial velocity) the stopping distance appears to be roughly the same for all D values we studied. We, therefore, take the values determined for $D = 10.3$mm as constant for all D.

Finally, the values of V_l for the different D values were evaluated as follows. The constant (i.e. independent of V) term of eqn. 4.3,

$$j = -\frac{V_l^2}{2K} + \frac{V_l}{a}\left(1 - \frac{V_{min}}{V_l}\right), \tag{4.5}$$

can be obtained directly, for each D, from the intersections of the fitted straight lines of $\tilde{L}$ versus V_i^2 with the vertical axis. The solution of eqn. 4.5 gives two values of $V_l(D)$, which are the two intersection points of equation 4.3 and 4.4. The smaller one is taken as the physical one corresponding to a passage from a more dissipative way to a less one. Fig. 8 shows the result of this analysis for all the studied values of D. Here we plot the experimental average stopping distance, $\tilde{L}$, as a function of the initial *velocity* (not $X_i \propto V^2$). The solid lines show the calculated values using equations 4.4 and 4.3. It can be seen that the agreement is very good. Note that since a and V_{min} have been taken as constants for all D, we only have two parameters left for adjustment to fit the data for the various D values. So, the very good agreement with experiments is obtained by tuning only two parameters.

D(mm)	2	3	4.7	6.3	7.1	10.3
K(m.s^{-2})	4.9	2.6	1.2	0.8	0.7	0.5
V_l(cm.s^{-1})	1.2	2.8	7.3	9.1	10.8	20.7

Table I. Values of the different parameters, for $\theta = 2^\circ$

The values of the parameters are given in table I. The value obtained for V_{min}, for the largest D, is consistent with zero: it is not possible to give a $\tilde{L}$ value acceptable when it is smaller than D, due to the measurements precision and the width of the distributions. We have obtained $a = 0.03s^{-1}$ for the prefactor in the viscous force while K and V_l values range between $500cm.s^{-2}$ and $50cm.s^{-2}$ and 1 cm/s and 21 cm/s, respectively, for values of D increasing from 4 to 20.6. It can be seen that the maximum value of the viscous deceleration, corresponding to the largest V_l, is around $0.6cm.s^{-2}$.

This means that a ball with $D = 10.3$mm which begins its motion over the rough surface with, for example, a velocity of 50 cm/s, "feels" a constant deceleration of $50cm.s^{-2}$ until it reaches a velocity of 21 cm/s. At that moment, the force *abruptly* becomes viscous and the deceleration decreases to $0.6cm.s^{-2}$. The velocity then continues to decrease and so does the friction force. When the velocity reaches the minimum value, V_{min}, the ball gets trapped.

This behaviour is easily motivated physically. When the ball is launched with a high velocity, collisions with the bumps on the surface cause it to undergo rather large bounces. The time of flight, dt, of these (ballistic) bounces is determined primarily by $V_\perp$ (the velocity normal to the surface), $dt \propto V_\perp$, and therefore the frequency of collisions is proportional to $V_\perp^{-1}$. With each collision the ball losses an amount of energy proportional to $V_\perp$, due to the coefficient of restitution. Therefore the energy lost per second, the product of these two quantities, is constant, i.e. a constant friction force. More elaborate calculations find similar results. [9]

At smaller velocities, the bounces are not high, the ball probes the geometry of the surface and the motion is a mixture of bouncing and rolling. The time of flight is, therefore, more complicated. The motion closely resembles that in the constant velocity regime thus giving viscous friction. The difference between this motion and the constant velocity regime, is that here the energy gained by the ball moving down the slope cannot compensate for the energy lost. The ball eventually gets pinned.

V_l appears like a limit velocity at which the ball can just "fly-over" the grains constituting the surface.

V. NUMERICAL SIMULATIONS

To investigate in more detail our conjectures concerning the motion of the particle we performed numerical simulations of the system. The motion of the particle was simulated using soft sphere molecular dynamics (for details see [15]). The sphere moves on a plane configuration scanned in from one of those used by Riguidel in his experiments [8]. As material parameters we use a normal coefficient of restitution $e_n = 0.6$ and a coefficient of friction of $\mu = 0.13$.

First we checked that we find the same global behaviour as in the experiments. Figure 9 shows the mean stopping distance, as averaged over the launching of 60 balls per starting velocity as a function of the initial kinetic energy. We find the same behaviour as in experiments – a linear region for higher starting velocities, and a not so well defined different shape of the curve for smaller starting velocities.

We now want to check whether the ball really covers the largest part of $\tilde{L}$ in large jumps. Figure 10 shows the distance covered between jumps as a function of time for different starting velocities. Obviously, the first part of the motion consists of very wide jumps (covering a few particle diameters at high starting velocities), but then drops very rapidly to much smaller distances. The times between collisions suddenly exhibit the very regular behaviour also observed in simulations of the steady state motion [15,16]: a number of small jumps, in the course of which all normal velocity with respect to the ball on the plane is lost, followed by a rolling over the rest of the ball. With the small angles of inclination and velocities in this case, this rolling starts very early on the ball, as is obvious from the long distances between collisions corresponding to them. In Fig. 11 the total distance covered in the same runs as in Fig. 10 is shown. Here, it becomes obvious that indeed, most of the $\tilde{L}$ is due to the large jumps at the beginning of the motion, and we see a very clearly defined crossover in the friction force. Only the curve corresponding to Fig. 10(a) does not exhibit this crossover. The reason is that the initial jumps were already not much longer than a particle diameter, since the initial velocity was quite low. Thus, the discrepancy between the two regimes of the motion is not very strong. Besides, the starting velocity corresponding to Fig. 10(a) is quite close to the lower limit of the linear region in Fig. 9, i.e. close to a different type of behaviour.

From Fig. 10 it is also obvious that the stopping *time* is very similar in all cases, but that the onset of rolling appears a bit later for higher starting velocities. As we assume in our physical model in section IV.B., stopping only takes place after the ball velocity has dropped below a certain value (in our case somewhere around 7 cm/s), at which point the rolling starts. This can be seen in Fig. 12, where we have plotted the evolution of the x-velocity of the ball for the same cases as in Fig. 10. The point where the ball starts to move in bounces much smaller than a ball radius (the stage prior to rolling) is marked with a small arrow for each trajectory.

It can also be seen from these curves that after a very rapid drop in the velocity after the first few collisions with the plane, the velocity seems to decrease in a linear fashion, though with a slope that seems to depend slightly on the initial velocity. Then, when the particle enters the phase of the motion consisting of a number of bounces with each

ball it passes (and eventually some rolling), the friction force experienced by the particle drops to a much lower value and seems to be independent of the initial velocity.

VI. CONCLUSION

We have investigated by means of experiments and numerical simulations the movement of a single ball on a rough inclined plane, at small inclination angle. This has given us a better understanding of the energy dissipation at small angles. We have shown that a ball which has a large enough initial velocity V_0 first bounces on the rough surface and suffers a constant friction force. Clearly in this case the ball cannot be trapped if its velocity is larger than the crossover velocity V_l. When the velocity reaches V_l, the friction force suddenly becommes viscous: the dynamics of the motion is now similar to that observed in regime B. The key for understanding these two mechanisms of dissipation, i.e. friction forces, is the difference in the nature of the collisions when the velocity is above or below V_l as explained above. We have also shown that the geometry of the surface plays an important role in the trapping of the ball. In regime A the ball is first slowed down gradually and when the velocity finally reaches a threshold value, V_{min}, (which appears to be *independent* of initial conditions) the ball is trapped. The trapping probability decreases linearly with the inclination of the plane. For the transition angle θ_T, this trappping mechanism disappears and the ball crosses over into the dynamic regime B where it moves on the plane with a constant mean velocity and is subjected to a viscous friction force [8,10]. In this regime, the ball can still be trapped by the occasional big defect on the surface but its trapping probability decreases *exponentially* with the angle of inclination. The fact that in both regimes A and B the friction force is viscous just before the ball gets trapped emphasizes the important fact that the difference between the two regimes A and B is not of dynamic origin, but due to two different trapping mechanisms.

The "divergence" of the median, L^*, of the stopping distance (defined as the length for which 50% of the balls are trapped) at θ_T is seen to indicate clearly the transition between the A and B regimes. The values of L^* depend on the initial velocity but the divergence always occurs at the same angle θ_T. This shows that the location of the transition is independant of initial kinetic energy. Numerical simulations gave us "microscopic" details of the motion (like the time between collisions) which agreed with and confirmed the experimental measurements and our explanations.

---

[1] J. Lee, Phys. Rev. E **49** 281 (1994)
[2] P. Bak, C. Tang and K. Wiesenfeld, Phys. Rev. Lett. **59**, 381 (1987)
[3] J. Duran, T. Mazozi, S. Luding, E. Clément and J. Rajchenbach, Phys. Rev. E **53**, 1923 (1996)
[4] E. Guyon and D. Bideau *Instabilities and Nonequilibrium Structures"*, Eds E. Tirapegui and W. Zellers, Kluvers Academics Publishers (1996)
[5] F. Heslot, T. Baumberger, B. Perrin, B. Caroli and C. Caroli, Phys. Rev. E **49**, 4973-4988 (1994)
[6] F. Radjai, P. Evesque, D. Bideau and S. Roux, Phys. Rev. E **52**, 5555 (1995)
[7] S. F. Foerster, M. Y. Louge, H. Chang and K. Allia, Phys. Fluids **6** (3), 1108 (1994)
[8] F. X. Riguidel, A. Hansen and D. Bideau, Europhys. Lett., **28**, 13 (1994).
[9] A. Valance and D. Bideau, Phys. Rev. E, submited.
[10] A. Aguirre, I. Ippolito, A. Calvo, C. Henrique and D. Bideau, Powd. Techn. **92**, 75-80 (1997).
[11] C. Henrique, M.A. Aguirre, A. Calvo, I. Ippolito and D. Bideau Powd. Techn., to appear.
[12] G. Batrouni, S. Dippel, L. Samson, Phys. Rev. E, **56**, 6496 (1996).
[13] S. Dippel, L. Samson, G. G. Batrouni in *Traffic and Granular Flow*, D. E. Wolf, M. Schreckenberg and A. Bachem (eds.) (World Scientific, Singapore 1996).
[14] S. Dippel, G. G.Batrouni, and D. Wolf, *Friction, Arching, Contact Dynamics*, and D. E. Wolf and P. Grassberger (eds.), World Scientific, Singapore, 1997.
[15] S. Dippel, G. G. Batrouni, D. E. Wolf, to appear in Phys. Rev. E.
[16] S. Dippel, G. G. Batrouni, D. E. Wolf, Phys. Rev. E **54**, 6845 (1996).

Figure 1. Histogram of the stopping distance for $D = 2mm$ (a) $\theta = 3°5$, (b) $\theta = 5°$, $X_i \approx 2mm$

Figure 2. Decay constant of the stopping distance distributions α as a function of the rough surface inclination angle θ, for $D = 2$mm.

Figure 3. Same as in figure 2 but obtained from the stochastic model, [12]

Figure 4. Median distributions, L^*, as a function of θ for $(\diamond)D = 10.3\text{mm}, (\circ)D = 3\text{mm}, (\triangleright)D = 1.6\text{mm}$

Figure 5. Variations of L^* with θ, for $D = 3\text{mm}$, and two initial velocities: $(\circ)V_i \approx 5$ cm/s and $(\bullet)V_i \approx 45$ cm/s.

Figure 6. Distributions of the stopping distance for $D = 10.3\text{mm}$, $\theta = 2^\circ$, and different initial square velocities $V_i^2 \propto X_i$, from left to right $X_i = 0.5, 4.5, 10.5, 16.5\text{cm}$

Figure 7. Average stopping distance $\tilde{L}$ as a function of $V_i^2 \propto X_i$, for $\theta = 2^\circ$, $(\triangle)D = 10.3\text{mm}$ and $(\circ)D = 4.7\text{mm}$

Figure 8. Average stopping distance $\tilde{L}$ as a function of V_i in arbitrary units, for $\theta = 2^\circ$, $(\triangle)D = 10.3\text{mm}$, $(\circ)D = 7.1\text{mm}$, $(\triangleright)D = 6.3\text{mm}$, $(\bullet)D = 4.7\text{mm}$, $(\triangleleft)D = 3\text{mm}$ and $(\diamond)D = 2\text{mm}$. In filled lines the calculated variation for the corresponding D values.

Figure 9. Average stopping distances for $D = 5$, $\theta = 1^\circ$.

Figure 10. Distance covered by the ball between sucessive collisions with the plane for three different starting velocities (a) $v_i = 20\text{cm/s}$, (b) $v_i = 30\text{cm/s}$, $v_i = 40\text{cm/s}$. The diameter of balls on the plane is 1 mm.

Figure 11. Total distance covered by the ball as a function of time for the same cases as in Fig. 10. Full line corresponds to (a), dashed line to (b), dot-dashed line to (c).

Figure 12. Velocity of the ball (same as in Fig. 10). Full line corresponds to (a), dashed line to (b), dot-dashed line to (c).

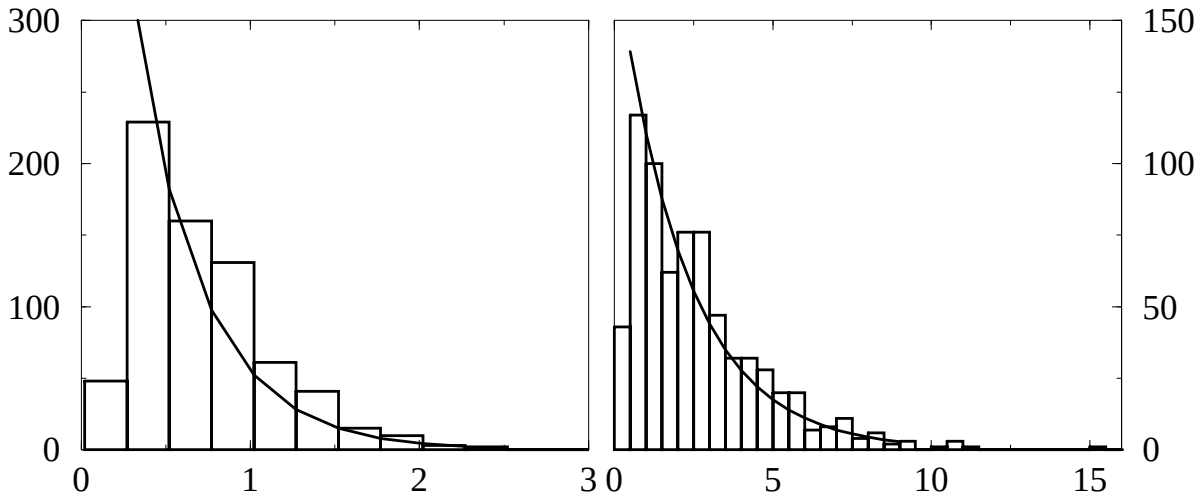

Figure 1

C. Henrique et. al.

‘‘Energy Dissipation and Trapping of Particles Moving on a Rough Surface’’

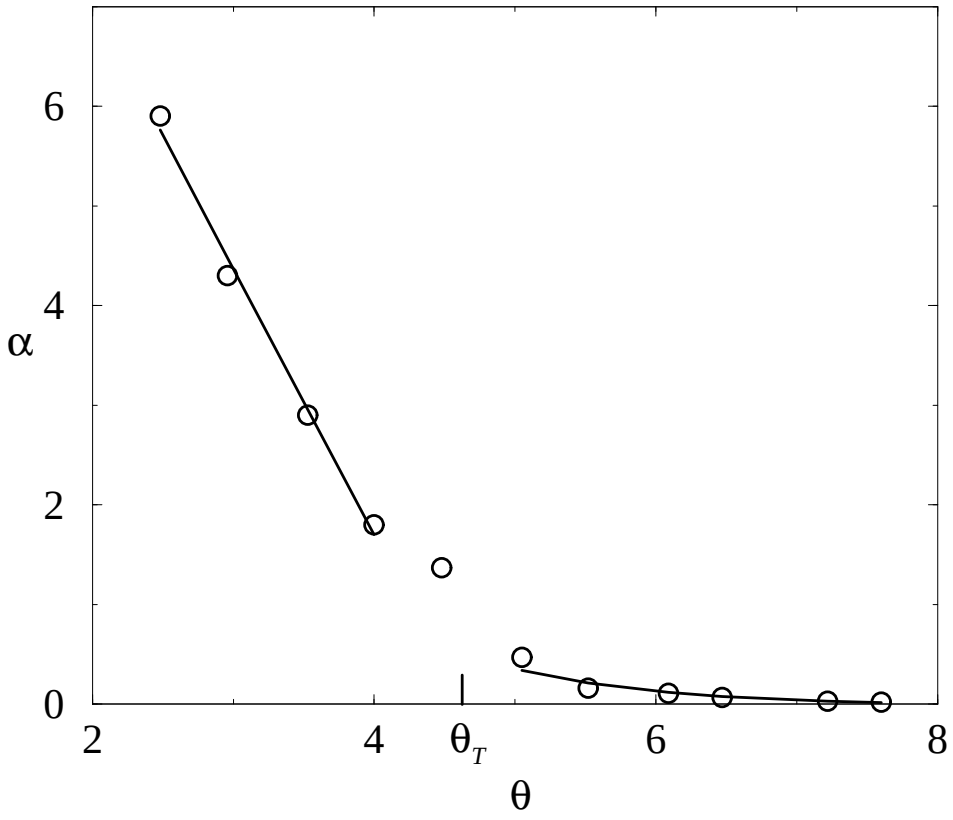

Figure 2

C. Henrique et. al.

''Energy Dissipation and Trapping of Particles Moving on a Rough Surface''

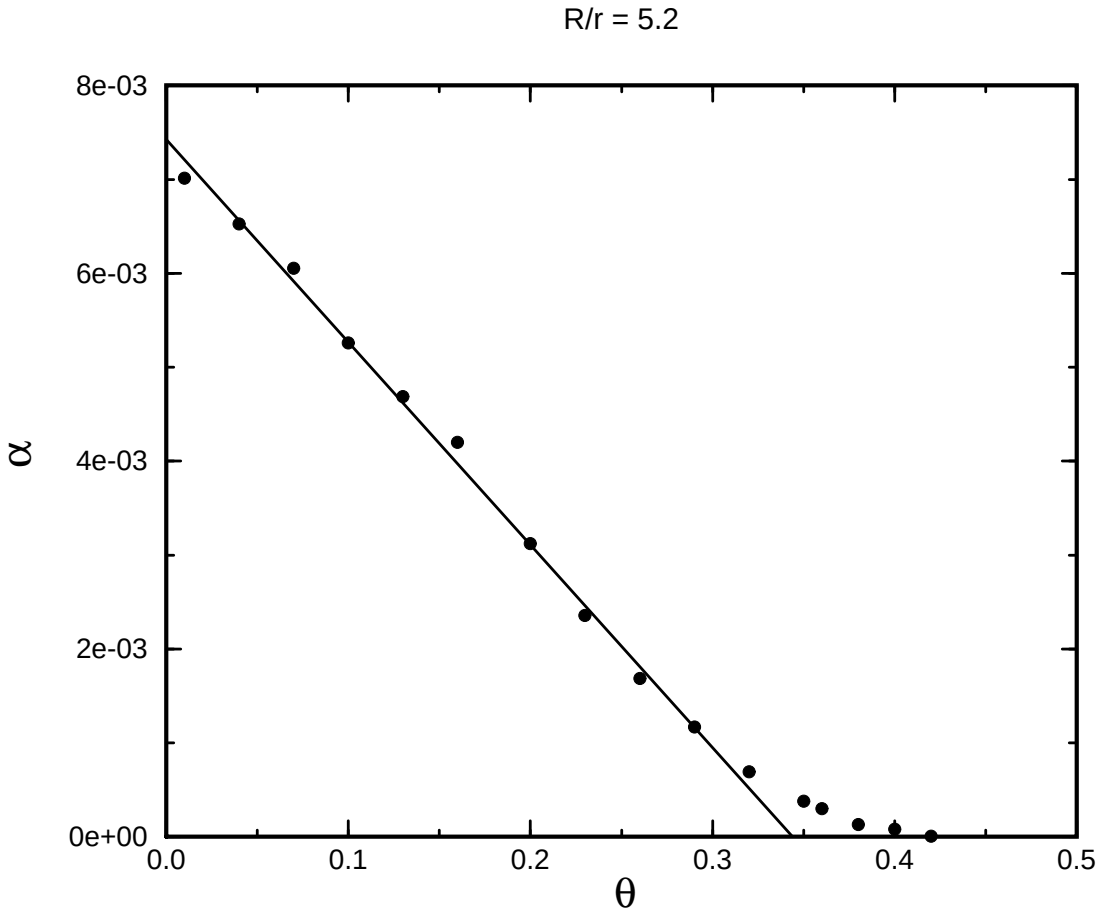

Figure 3

C. Henrique et. al.

‘‘Energy Dissipation and Trapping of Particles Moving on a Rough Surface’’

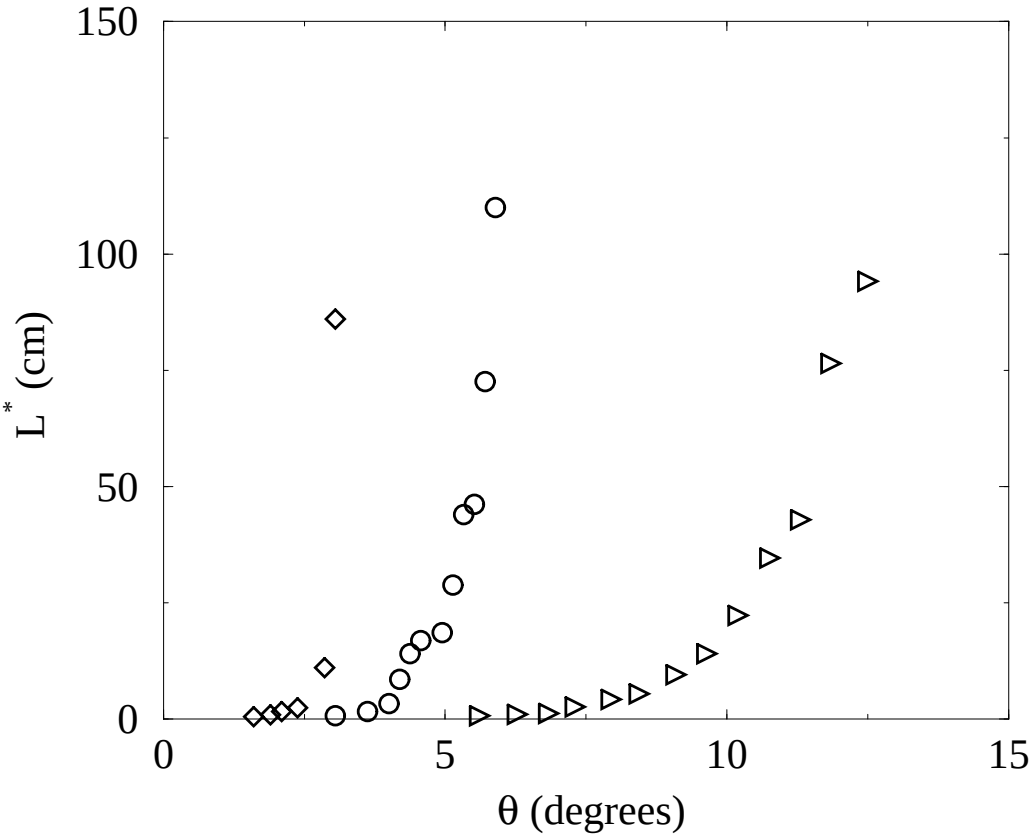

Figure 4

C. Henrique et. al.

''Energy Dissipation and Trapping of Particles Moving on a Rough Surface''

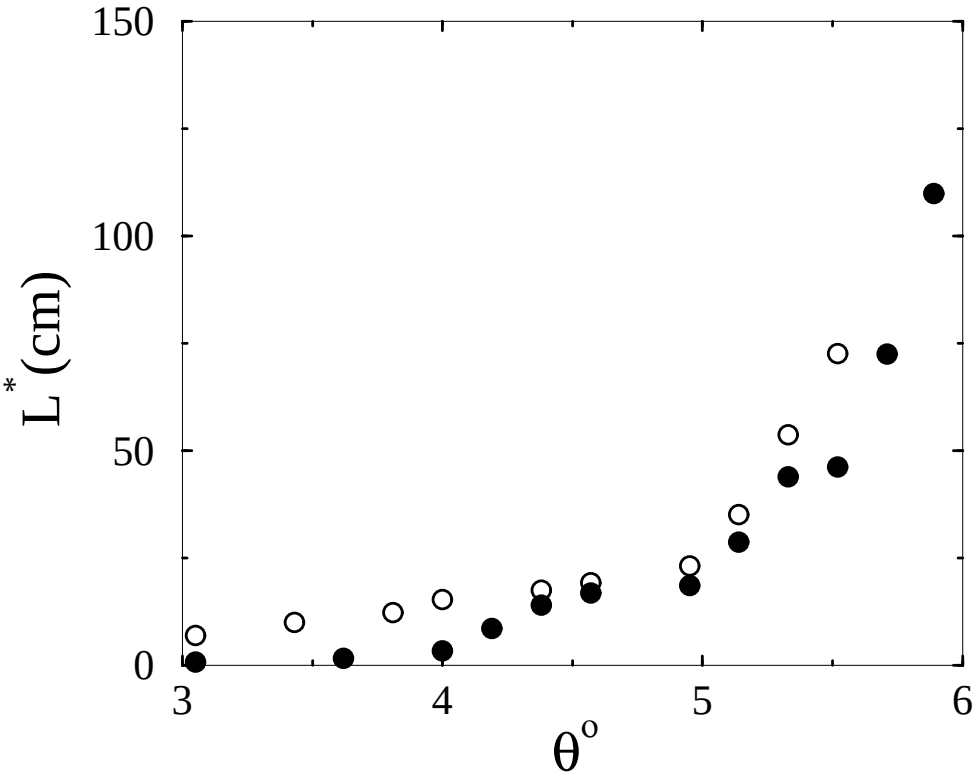

Figure 5

C. Henrique et. al.

''Energy Dissipation and Trapping of Particles Moving on a Rough Surface''

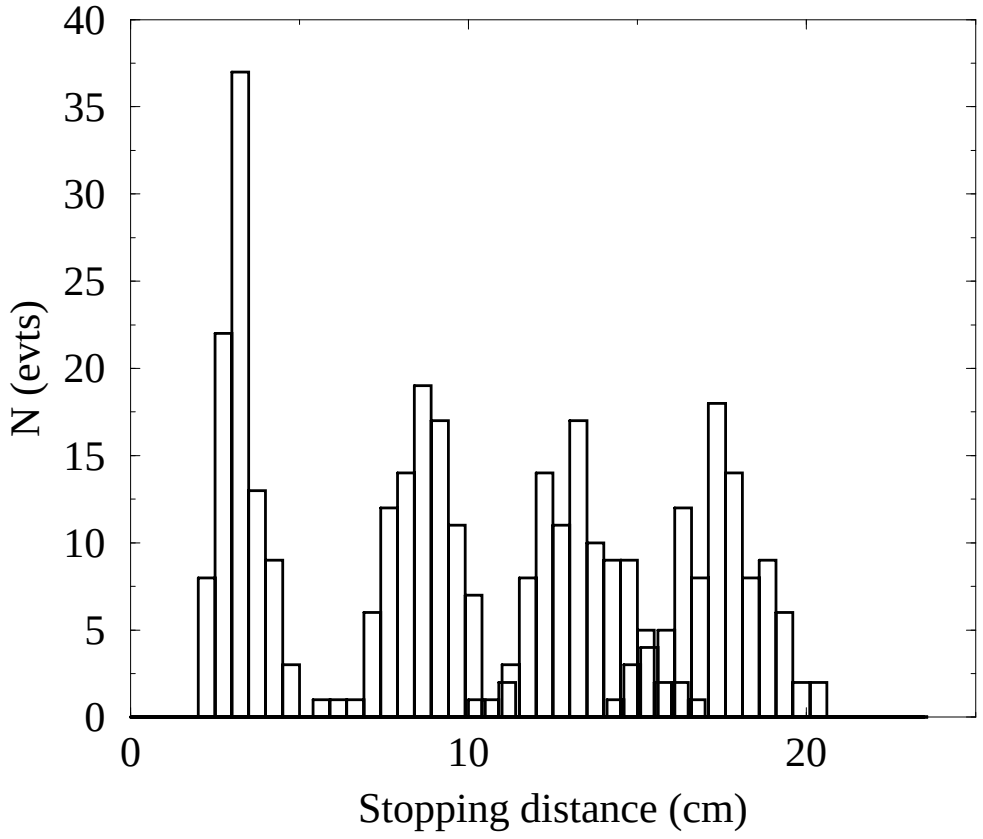

Figure 6

C. Henrique et. al.

''Energy Dissipation and Trapping of Particles Moving on a Rough Surface''

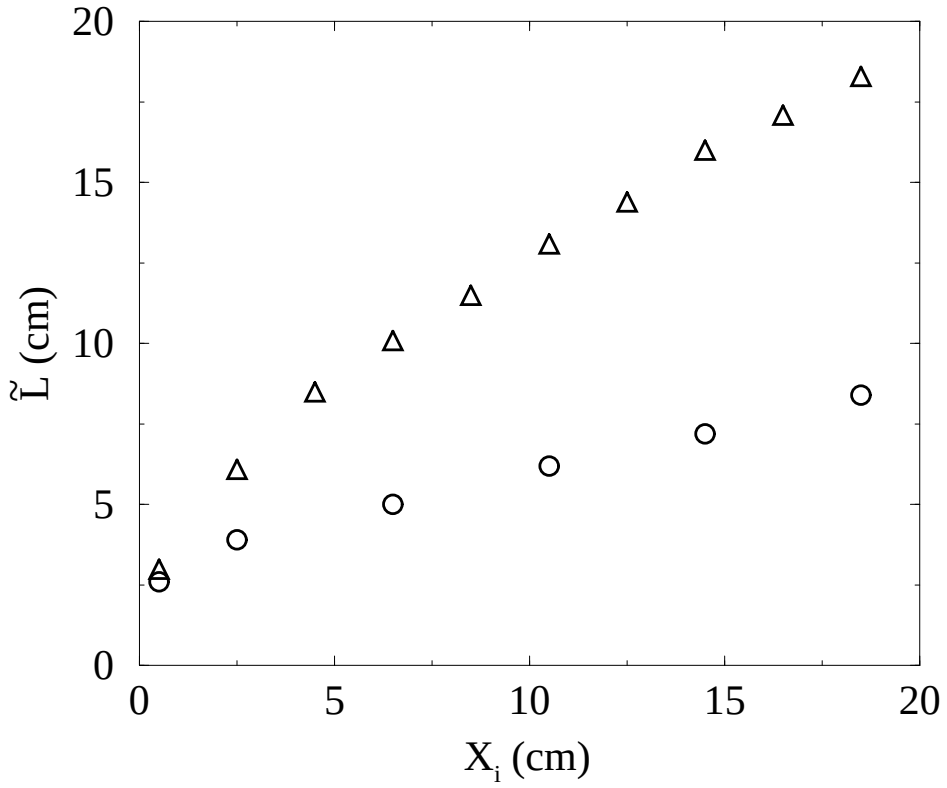

Figure 10

C. Henrique et. al.

‘‘Energy Dissipation and Trapping of Particles Moving on a Rough Surface’’

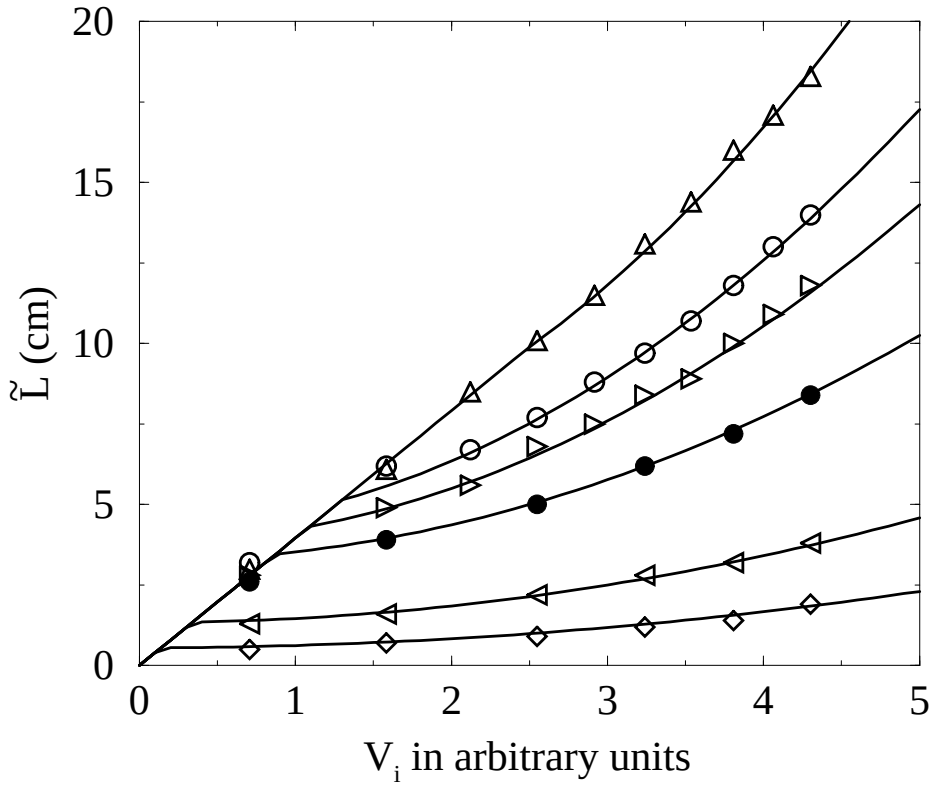

Figure 8

C. Henrique et. al.

''Energy Dissipation and Trapping of Particles Moving on a Rough Surface''

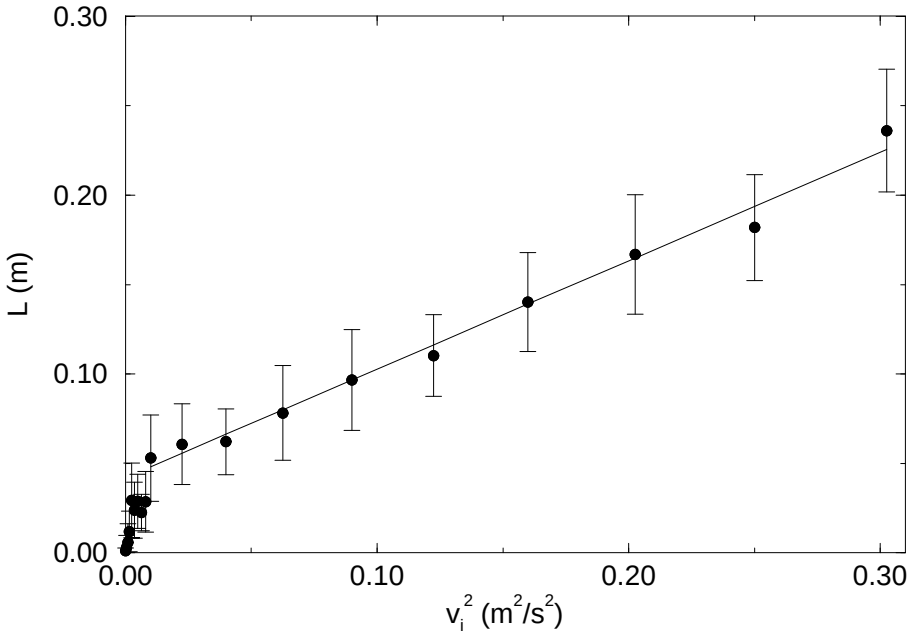

Figure 9

C. Henrique et. al.

''Energy Dissipation and Trapping of Particles Moving on a Rough Surface''

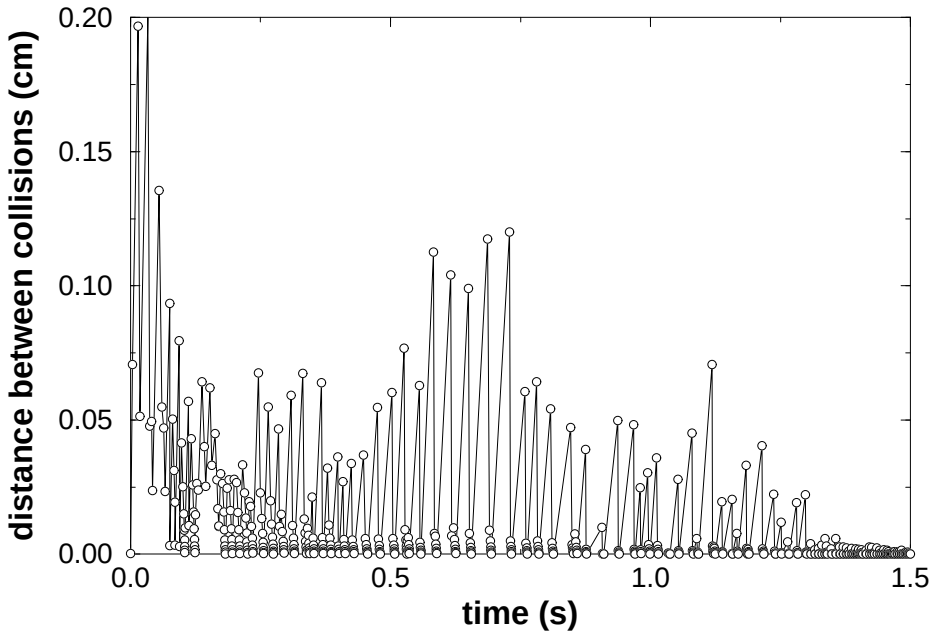

Figure 10 (a)

C. Henrique et. al.

''Energy Dissipation and Trapping of Particles Moving on a Rough Surface''

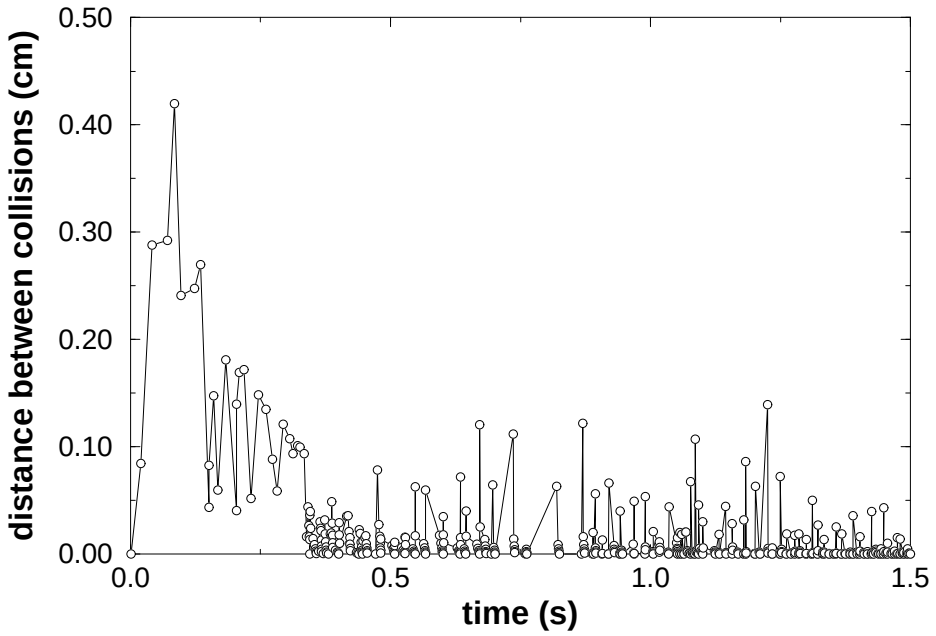

Figure 10 (b)

C. Henrique et. al.

''Energy Dissipation and Trapping of Particles Moving on a Rough Surface''

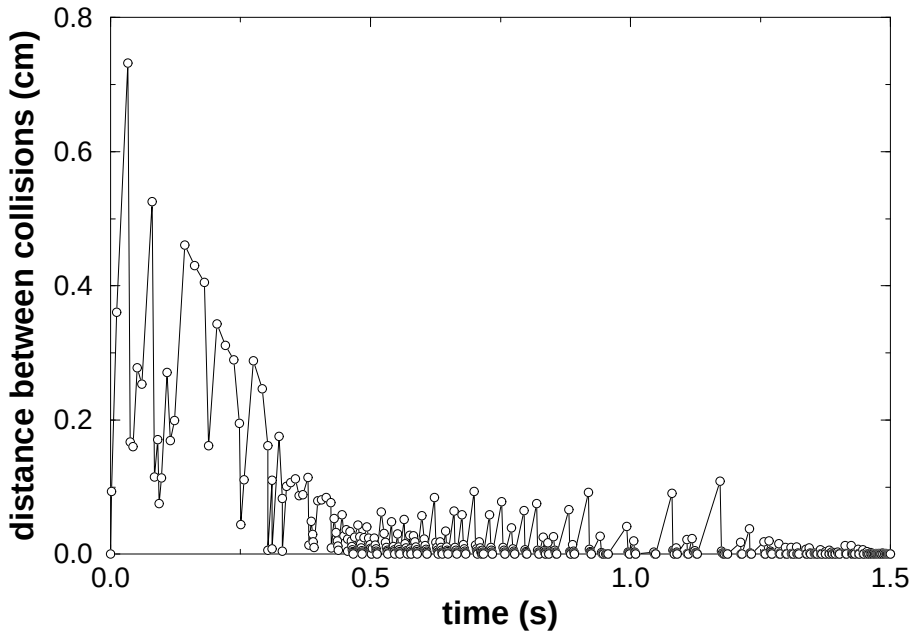

Figure 10 (c)

C. Henrique et. al.

‘‘*Energy Dissipation and Trapping of Particles Moving on a Rough Surface*’’

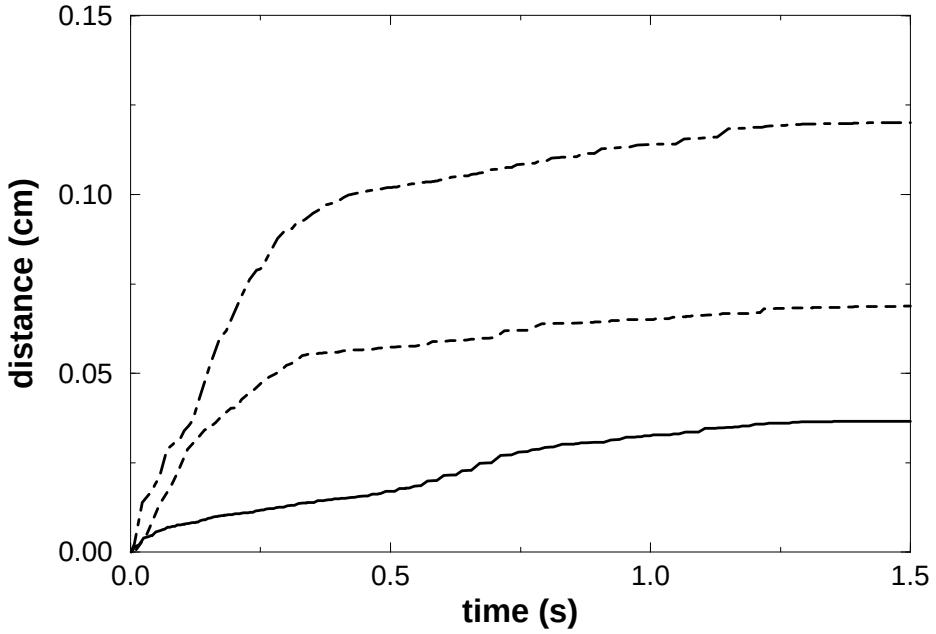

Figure 11

C. Henrique et. al.

''Energy Dissipation and Trapping of Particles Moving on a Rough Surface''

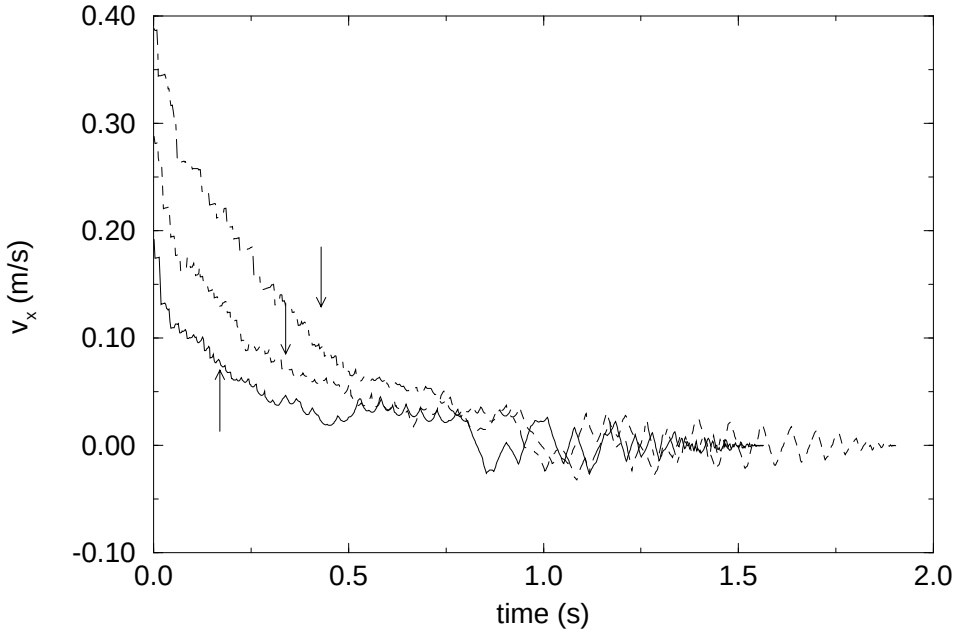

Figure 12

C. Henrique et. al.

‘‘Energy Dissipation and Trapping of Particles Moving on a Rough Surface’’